

# Reducing Motion Artifact in Wearable Bio-Sensors Using MEMS Accelerometers for Active Noise Cancellation

Peter Gibbs and H. Harry Asada, *Member, ASME*

**Abstract**—This paper presents an active noise cancellation method using a MEMS accelerometer that recovers wearable sensor signals corrupted by body motion. The method is developed for a finger ring photoplethysmograph (PPG) sensor, the signal of which is susceptible to the hand motion of the wearer. A MEMS accelerometer (ACC) imbedded in the PPG sensor detects the hand acceleration, and is used for recovering the corrupted PPG signal, based upon two different methods of modeling the process of signal corruption. The correlation between the acceleration and the distorted PPG signal is analyzed, and a low-order FIR model relating the signal distortion to the hand acceleration is obtained. The model parameters are identified in real time with a recursive least square method. Experiments show that the active noise cancellation method can recover ring PPG sensor signals corrupted with 2G of acceleration in the longitudinal direction of the digital artery.

## I. INTRODUCTION

Wearable biosensors are expected to be revolutionary in many application areas, ranging from cardiovascular monitoring to battle field monitoring and sports medicine [1]. However, reliability of these wearable sensors is by far inferior to their traditional counterparts, leading to frequent false alarms [2]. Since most of the potential applications are for field use, the wearable sensors must be robust against disturbances, in particular, the motion of the wearer. New technology is needed for eliminating motion artifact and recovering signals corrupted with the body motion.

Accelerometers have long been used for monitoring daily activities of elderly people and rehabilitation patients, as well as for clinical monitoring for COPD and others [3, 4]. In this paper, a new method for creating motion tolerant wearable sensors using MEMS accelerometers will be presented. In the following, the method will be developed in the context of reducing motion artifact in a photoplethysmograph (PPG) ring sensor [5]. First, the

integrated PPG/ACC system design implementing two different signal distortion models is described, followed by a description of the correlation analysis between acceleration and PPG distortion. An active noise cancellation algorithm will then be developed, and experiments will show the effectiveness of the proposed methods.

## II. MOTION ARTIFACT REDUCTION THEORY

### A. Additive Distortion Model [6].

Any physiological measure, such as pulse or blood pressure wave, is distorted when subjected to body motion. Any wearable biosensor attempting to measure such a signal will therefore be detecting a mixture of both the true signal and a distorted signal. The simplest modeling of this situation, assumes these two signals to be additive. With this assumption, Fig. 1 shows the principle of a motion-tolerant wearable biosensor using a MEMS accelerometer, with the true signal labeled  $y_o$  and the distorted signal labeled  $w$ . The body motion is detected with a MEMS accelerometer incorporated into the biosensor. An adaptive filter estimates the dynamics of the distortion process, and produces the estimate of the distorted signal  $\hat{w}$  in response to the measured acceleration  $a$ . The estimated distortion  $\hat{w}$  is then subtracted from the biosensor output  $y$ . The adaptive filter comprises a dynamic model predicting how the distorted signal component is generated in response to the body acceleration. The model parameters are estimated in real-time such that the recovered signal may have a minimum variance. The details of this process will be discussed in the Methods section of the paper.

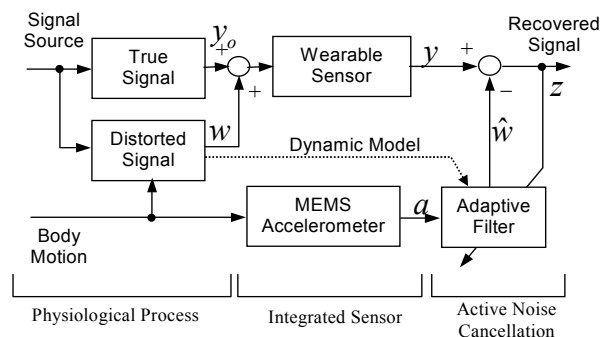


Fig. 1 Block diagram of motion-tolerant wearable bio-sensor system with built-in accelerometer and active noise cancellation filter assuming distorted signal is additive

Manuscript Received August 27, 2004. This work is supported by National Institute of Health Grant, No. 1 R21 EB002258-01. The analytic aspect of the work is supported by the National Science Foundation under Grant No. NSF CMS-0330280.

Peter Gibbs is a graduate student and H. Harry Asada is a professor at the Massachusetts Institute of Technology, Cambridge, MA 02139 USA email: asada@mit.edu.

### B. Multiplicative/Logarithmic Distortion Model

While the simplest model assumes the combination of the true signal and the distorted signal is additive, there is reason to believe this may not accurately model the actual dynamics taking place in the system. The distortion process may in fact be “multiplicative”, rather than additive in the case of a PPG sensor. This idea follows from knowing the light intensity received at the photodiode of a PPG sensor obeys Beer’s Law [7]:

$$y = \alpha e^{-\epsilon d} \quad (1)$$

where  $y$  is the light intensity (signal received) at the photodiode,  $\alpha$  is the intensity at the LED source,  $\epsilon$  is the absorption/extinction coefficient (dependent on the light wavelength and nature of the absorbing medium), and  $d$  is the distance between the light source, and the photodiode. In a firmly attached PPG sensor,  $\alpha$  is assumed constant, while changes in  $\epsilon$  and  $d$  are primarily caused by the pulsatile dynamics of the blood vessels in the body. Unfortunately, body motion can cause changes in these two parameters as well, leading to signal corruption. In particular, acceleration of the finger in the longitudinal direction will cause changes in the diameters of the digital arteries; changes which are completely unrelated to the desired physiological measures.

Let us now combine the parameter  $\epsilon d$  into a single parameter,  $K$ . We further subdivide  $K$  into two separate components, which we assume to be additive:  $K_{PPG}$  and  $K_{ACC}$ .  $K_{PPG}$  corresponds to the true PPG signal we desire to capture, and  $K_{ACC}$  corresponds to changes caused by the acceleration of the finger alone. With these new assumptions, (1) can be written as

$$y = \alpha e^{-(K_{PPG}+K_{ACC})} = \alpha e^{-K_{PPG}} e^{-K_{ACC}} = y_o k \quad (2)$$

where the desired true PPG signal is  $y_o$  and the part of the signal due to distortion is  $k$ .

Taking the natural logarithm of both sides of (2), we have the following equality

$$Y = Y_o - K_{ACC} \quad (3)$$

where  $Y$  and  $Y_o$  are the logarithmic transforms of  $y$  and  $y_o$ .

The modeled system is now in a form suitable for the adaptive noise cancellation process. Fig. 2 shows the principle of a motion-tolerant wearable biosensor system using this new modeling approach.

## III. METHODS

### A. Integrated PPG/ACC Ring Sensor

Fig. 3 shows an initial embodiment of a motion-tolerant wearable biosensor. The wearable sensor is a PPG ring sensor, measuring pulse and saturated oxygen level at the finger base. The ring sensor signal is often distorted significantly due to the hand motion. In particular, motion in the longitudinal direction of the finger causes a serious distortion of the PPG signal, since the digital artery runs in the same direction. To detect this acceleration, a MEMS accelerometer is incorporated into the PPG ring sensor, so that both sensors detect signals at the same point.

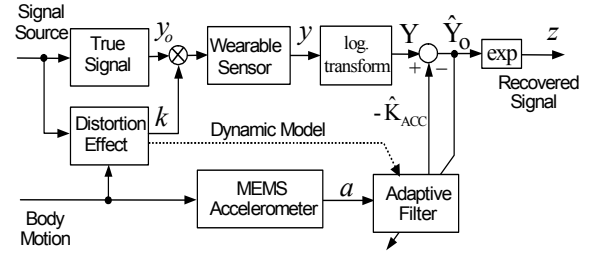


Fig. 2 Block diagram of motion-tolerant wearable bio-sensor system assuming distortion effect is multiplicative

### B. Correlation Analysis

Prior to designing the adaptive filter for active noise cancellation, the correlation between the finger acceleration and the distortion of the PPG signal was analyzed based on experiments using the integrated PPG/MEMS-ACC ring sensor. Fig. 4 shows preliminary experimental results from the ring sensor worn by a jogger running on a treadmill. The bottom signal waveform (a) is the MEMS accelerometer output (1 Volt = 10 G acceleration) when the jogger swung the left hand with the ring sensor attached. The second from bottom waveform (b) is the corrupted PPG signal, which strongly correlates with the acceleration. For comparison, a second PPG sensor (Nellcor PPG) was attached to the right hand of the jogger, which was kept stationary during the experiment. The top waveform (c) is this control PPG signal measured from the stationary hand. (Please note all PPG signals have been shifted vertically on the plot for presentation purposes). The dotted vertical line indicates the timing of the first peak of each pulse, from which pulse rate is determined. The corrupted PPG ring sensor signal not only differs in waveform from the stationary PPG signal, but the timing of the first peak also differs significantly from the stationary PPG.

Denoting the corrupted PPG data series from the moving hand as  $y_t$  and the correct PPG from the stationary hand as  $y_{o,b}$  we can define the approximate signal distortion series using the additive distortion model as:

$$\hat{w}_t = y_t - y_{o,t} \quad (4)$$

Using this model in the correlation analysis, we have assumed that in the experiment, the correct PPG signal obtained at the stationary hand is approximately equal to the correct PPG signal that would have been obtained from the moving hand had it been stationary. While in actuality,

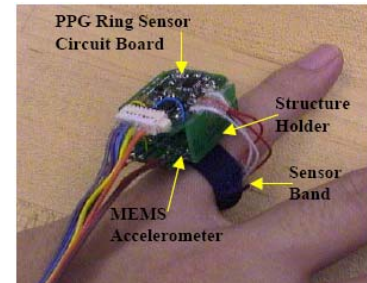


Fig. 3 Prototype of integrated PPG/MEMS-ACC ring sensor

TABLE I

Correlation of delayed  $\tilde{w}$  series with the  $a$  series (strongest highlighted)

a-series Test No.	Corrupted PPG – Correct PPG ( $\tilde{w}$ -series)					
	No delay	+0.07s delay	+0.08s delay	+0.09s delay	+0.10s delay	+0.11s delay
1	0.28	0.86	0.89	0.89	0.88	0.86
2	0.05	0.90	0.93	0.92	0.89	0.83
3	0.18	0.92	0.93	0.92	0.88	0.81
4	-0.30	0.67	0.74	0.78	0.79	0.77
5	-0.15	0.72	0.78	0.81	0.81	0.79
6	0.02	0.74	0.78	0.81	0.81	0.79

movement of one arm will indeed affect vascular dynamics throughout the rest of the body, including the stationary hand, these effects are believed to be minimal, thus enabling us to proceed in this manner.

Table I shows the correlation between the accelerometer signal,  $a_t$ , and the signal distortion,  $\tilde{w}_t$ , sampled with a 1 ms sampling interval from an experiment repeated six times. Each experiment continued for 25 sec, i.e. 25,000 samples, and the hand was moved in various ways during the course of the experiment. From these results, it is seen that there is a significant time lag in the response of the corrupted PPG signal to the acceleration. The delay is the time between supplying an input acceleration and observing a significant alteration to the PPG signal from that acceleration. The reason for this delay is due to many physical factors within the digit, but may be partially as a result of the fluid inertance and the vasculature capacitance.

To quantify this time lag, we have evaluated the correlation between the accelerometer signal,  $a_i$ , and delayed PPG distortion,  $\tilde{w}_{i+d}$ :

$$Cor(\tilde{w}, a; d) = \frac{1}{m} \frac{\sum_{i=1}^m (\tilde{w}_{i+d} - \mu_{\tilde{w}})(a_i - \mu_a)}{\sigma_{\tilde{w}}\sigma_a} \quad (5)$$

where  $\mu, \sigma$  are the mean and the standard deviation of each of the signals respectively. As shown in the second column of Table 1, the correlation is low when no time delay is involved,  $d=0$ . As time delay  $d$  increases, a high level of correlation is observed over a particular range.

Fig. 5 shows more clearly how the correlation depends on the time delay  $d$ . Shown in this figure is both the

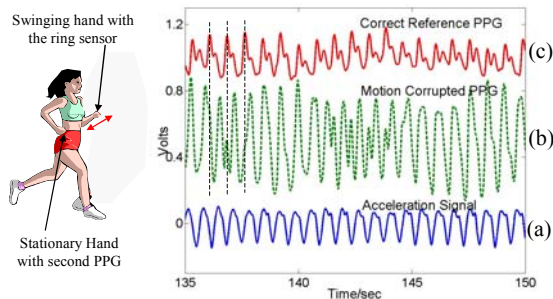


Fig. 4 Experiment of PPG ring sensor, control PPG, and MEMS accelerometer for jogger monitoring.

correlation between  $\tilde{w}$  and  $a$  (additive model), and the correlation between  $\tilde{K}_{ACC}$  and  $a$  (logarithmic model), with  $\tilde{K}_{ACC}$  defined for the logarithmic case analogous to how  $\tilde{w}$  was defined for the additive case. It is clear that for both models, the correlation is high for a certain time window, and then it decreases as  $d$  is further increased. From this data and correlation analysis, we gain insights as to how acceleration influences the PPG signal and how the dynamic process can be modeled effectively:

- The longitudinal acceleration is strongly correlated with the corrupted PPG signal. This implies that the corrupted PPG signal can be predicted from the measured acceleration.
- A high level of correlation is observed only for a limited time window. This implies that the dynamic response is finite and that the dynamic relationship can be described as a finite time series, such as FIR (Finite Impulse Response).
- A reduced-order FIR model may be obtained by tuning parameters specifically to the limited time window of high correlation.

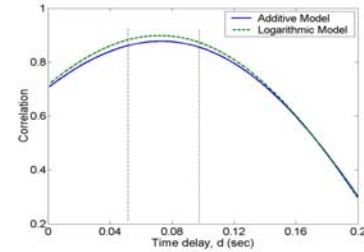


Fig. 5 Plot of Correlation index between signal distortion series and acceleration series against time delay in signal distortion series (results shown for a typical test)

### C. Active Noise Cancellation Methodology

Based on the above correlation analysis, a dynamic model predicting the distortion of the PPG ring sensor signal in response to acceleration has been built. The model is a Finite Impulse Response type with a specific time window having high correlation with the acceleration signal. The FIR coefficients are then estimated in real-time to minimize the variance of the recovered signal.

As shown in Fig. 1 for the additive model case,  $y_o$  is the true PPG signal and  $w$  is the distorted signal component added to the true signal. The actual PPG sensor output  $y$  is a corrupted one given by  $y = y_o + w$ . Let  $\hat{w}$  be an estimate of the distorted signal component to be created by the adaptive filter. The objective of the adaptive filter is to minimize the error  $w - \hat{w}$ . This can be achieved by evaluating the signal power of the recovered signal  $z = y - \hat{w}$ :

$$E[z^2] = E[(y_o + w - \hat{w})^2] \quad (6)$$

$$= E[y_o^2] + 2E[y_o w] - 2E[y_o \hat{w}] + E[(w - \hat{w})^2].$$

Note that the true PPG signal  $y_o$  is uncorrelated with the body motion and thereby uncorrelated with the distorted

signal component  $w$  and its estimate  $\hat{w}$ . Therefore, the second and the third terms in the above equation vanish *as long as*  $y_o$  has a zero mean. (A method for satisfying this requirement will be discussed in the next section). In consequence, minimizing  $E[z^2]$  is equivalent to minimizing  $E[(w - \hat{w})^2]$ , since the first term  $E[y_o^2]$  is irrelevant to minimization with respect to the filter coefficients. This is essentially Widrow's Active Noise Cancellation (ANC) [8]. The above algorithm does not assume prior knowledge of the values of process parameters, but it continuously adjusts the model parameters to minimize the error between  $y$  and  $y_o$  through minimizing the power in  $z$ .

Similarly, for the multiplicative model (see Fig. 2), we wish to minimize the error  $K_{ACC} - \hat{K}_{ACC}$ . Looking at the signal power of the recovered signal,  $\hat{Y}_o$ :

$$E[\hat{Y}_o^2] = E[Y_o^2] + 2E[Y_o K_{ACC}] - 2E[Y_o \hat{K}_{ACC}] + E[(K_{ACC} - \hat{K}_{ACC})^2] \quad (7)$$

we can now minimize the error by minimizing  $E[\hat{Y}_o^2] = E[(Y - \hat{K}_{ACC})^2]$ , as long as  $Y_o$  has a zero mean.

#### D. Mean Shifting Algorithms

In the preceding section, it was noted that the active noise cancellation algorithm requires the following:  $E[y_o] = 0$  for the additive case, and  $E[Y_o] = 0$  for the logarithmic case. We will now look at how to satisfy this constraint; first for the additive case, and then for the logarithmic case.

Since  $y_o$  is the true signal, which is unknown, it is not possible to explicitly guarantee that it has a zero mean. It is possible, though, to shift the corrupted output signal  $y$  so that it has a zero mean over an arbitrary length of time. This shifted signal can be written as:

$$\bar{y} = y - E[y], \quad (8)$$

such that  $E[\bar{y}] = 0$ . We can now use this shifted signal in the ANC algorithm to minimize  $E[(\bar{y} - \hat{w})^2]$ . If we assume the signal corruption  $w$  has a zero mean (since the average hand acceleration over time is approximately zero), then it follows that  $\bar{y}_o = \bar{y} - w$  also has a zero mean over the arbitrary length of time defined for  $\bar{y}$ . Therefore, the error  $w - \hat{w}$  can now be successfully minimized. The recovered signal is:

$$\bar{z} = \bar{y} - \hat{w} \quad (9)$$

The estimate of the true, original signal is then found by re-shifting the signal:

$$\hat{y}_o = \bar{z} + E[y] \quad (10)$$

For the logarithmic case, analogous operations must be performed. In this case,  $Y$  is shifted to have a zero mean, motivated by similar assumptions as before:

$$\bar{Y} = Y - E[Y] \quad (11)$$

As in the additive case, we can then recover the signal,  $\hat{Y}_o$ , which leads to an estimate of the original signal:

$$\hat{y}_o = \exp(\hat{Y}_o) = \exp(\bar{Y}_o + E[Y]). \quad (12)$$

#### E. FIR Filter Parameters

The process parameters to identify are the FIR coefficients generating the estimate of distorted signal  $\hat{w}$  ( $\hat{K}_{ACC}$  in the logarithmic case):

$$\hat{w}_t = \theta_t^T \cdot \varphi_t, \quad (13)$$

where

$$\theta_t = (q_1 \quad q_2 \quad \dots \quad q_n)^T$$

$$\varphi_t = (a_{t-d} \quad a_{t-d-1} \quad \dots \quad a_{t-d-n+1})^T.$$

The regressor  $\varphi_t$  consists of a delayed time sequence of measured acceleration,  $a_{t-d} \quad a_{t-d-1} \quad \dots \quad a_{t-d-n+1}$ . Note that  $q_i$  is the  $i$ -th FIR parameter and  $n$  is the number of parameters, i.e. the model order. These parameters are determined in real time to minimize the signal power,  $z$  ( $\hat{Y}_o$  in the logarithmic case). This parameter estimation can be performed with various real-time computation algorithms, including the standard Recursive Least Squares (RLS), which was implemented in this study.

Both the values of  $d$  and  $n$  are the two most important issues in designing the FIR filter. The model order,  $n$ , must be chosen such that the time window is large enough to accurately model the system, while remaining a reasonable order to allow for real time computation. Likewise, the time delay,  $d$ , must be chosen such that the filter captures the acceleration signals that most affect the current PPG signal. These issues will be explored further in the Experimental Results section.

## IV. SIMULATION RESULTS

The ANC algorithms were first implemented on a sine wave signal ( $y_o$ ), corrupted by a simulated distortion signal ( $w$  or  $K_{ACC}$  depending on the model used). The resulting corrupted signal ( $y$ ) was input into the appropriate ANC/RLS algorithm and a reconstructed signal ( $\hat{y}_o$ ) was obtained. An arbitrary acceleration signal ( $a$ ), shown in Fig. 6 was used as the source of the signal corruption.

In each simulation, the values for  $w$  or  $K_{ACC}$  were determined from the acceleration signal using an FIR filter of order 100, with constant, arbitrarily chosen parameters. The ANC algorithm was implemented assuming an adaptive FIR filter of order 100, but with no initial knowledge of the filter parameters. Fig. 7 shows the results of a simulation using the additive distortion model. In this case, the mean of the original signal ( $y_o$ ) was zero, and the resulting reconstruction is quite good. Fig. 8, on the other hand, shows the results of a simulation where  $E[y_o] \neq 0$ .

As is seen from Fig. 8(b), if  $y$  is not shifted to have a zero mean before implementing the ANC/RLS algorithm, a poor reconstruction results. When  $y$  is shifted, though, an acceptable reconstruction is obtained.

Figure 9 shows similar results for a logarithmic model simulation. In this case as well, an accurate reconstruction

is obtained if the appropriate mean shifting algorithms are implemented as explained in the previous section.

## V. EXPERIMENTAL RESULTS

The active noise cancellation method using the MEMS accelerometer was then implemented and tested in physical experiments using the PPG ring sensor on a jogger on a treadmill. Fig. 10 shows experimental results using both of the models, with delay time of  $d=80$ , i.e. 80 ms, and an FIR model order of  $n=10$ . The left hand with the ring sensor was shaken at different accelerations, as shown in (a). The recovered PPG signals (d) and (e) both correctly show the first peak in every heart beat even under a large acceleration, i.e. more than 2 G. Note that every peak time completely agrees with that of the control PPG signal (c) from the stationary hand, although the motion-corrupted signal in (b) shows a totally different peak time in most heart beats. These results indicate the apparent effectiveness of both models in reconstructing the main peak of the waveform. The logarithmic model appears to do a slightly better job, though, of capturing the overall shape of the original signal, as seen in Fig. 11. In this figure, the reconstructed waveforms have been shifted and scaled in the magnitudinal direction (which is not of concern in the absolute sense in PPG analysis) for a better comparison. Using the logarithmic model, the first and second peaks are both fairly well defined, with the proportional size of each more comparable to the correct PPG signal than in the additive case. Therefore, the remaining plots were all created using the logarithmic/multiplicative distortion model. The FIR filter order,  $n$ , was chosen as 10 for these experiments. A low order model was chosen to decrease computation time, and a filter order even as low as 10 was capable of accurately recovering the signal.

From the correlation analysis, it was determined that a delay of approximately 80 ms gave the highest correlation between the acceleration signal and the PPG distortion. Fig. 12 shows the results of attempting to reconstruct the PPG signal with multiple delays ( $n=10$  in each case). In constructing this plot, the peak times from the reconstructed signals were found, and compared to the corresponding peak times of the “correct” reference signal. The average rms error between these two times was calculated for eight different delays in the FIR filter. As can be seen, the minimal error occurred when a delay of 75-80 ms was implemented.

Choice of a sampling rate is another important design issue. Fig. 13 shows recovered PPG signals using the logarithmic model for diverse sampling rates. The experimental results show that the waveform is adequately recovered even for a reduced sampling rate of 100 samples/sec.

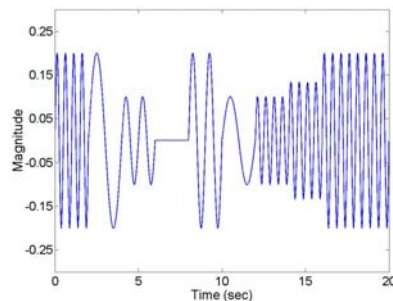


Fig. 6 Acceleration signal used in simulations

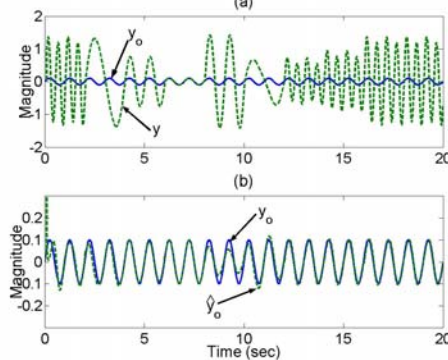


Fig. 7 Use additive model on zero mean original signal: (a) Compared with corrupted signal;  $y$ ; (b) Compared with reconstructed signal,  $\hat{y}_o$

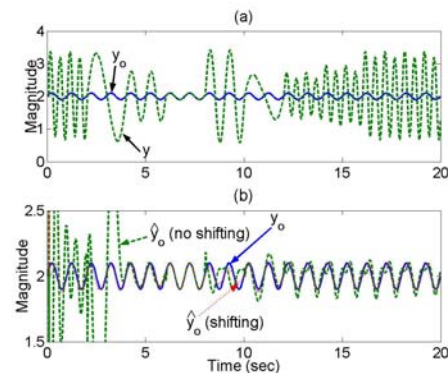


Fig. 8 Using additive model on non-zero mean original signal: (a) Compared with corrupted signal;  $y$ ; (b) Compared with reconstructed signals,  $\hat{y}_o$  both using and not using the mean shifting algorithm

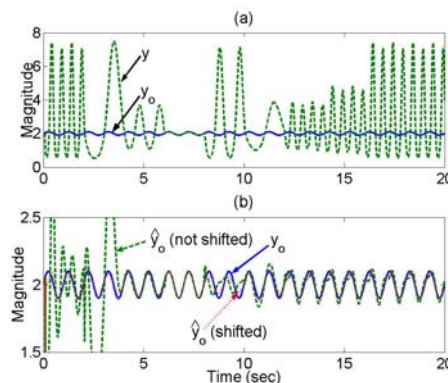


Fig. 9 Using logarithmic model on non-zero mean original signal: (a) Compared with corrupted signal;  $y$ ; (b) Compared with reconstructed signals,  $\hat{y}_o$  both using and not using the mean shifting algorithm

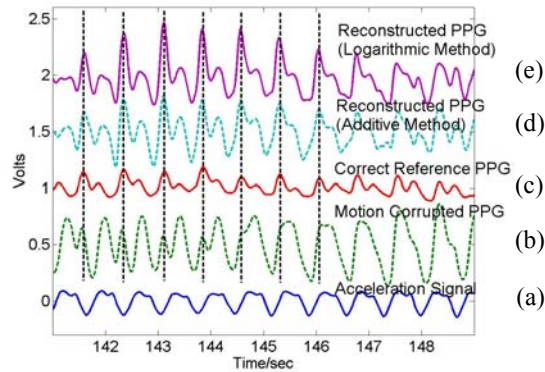


Figure 10 Comparing the reconstructed PPG with the correct reference PPG using (d) the additive distortion model and (e) the logarithmic/multiplicative model

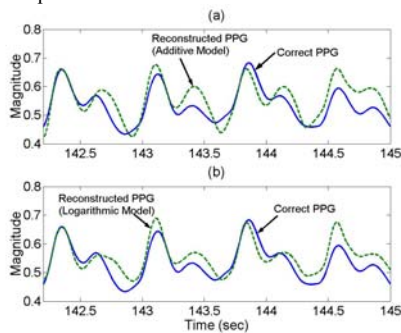


Fig. 11 Comparing waveform shape by superimposing reconstructed waveform over correct waveform for the (a) additive model case and (b) logarithmic model case

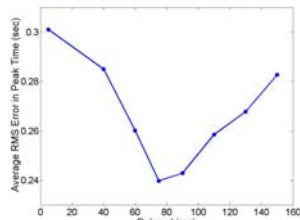


Fig. 12 Average rms error in signal peak time for different time delays used in FIR model (filter order  $n=10$  kept constant,  $d$  varies from 5 to 150)

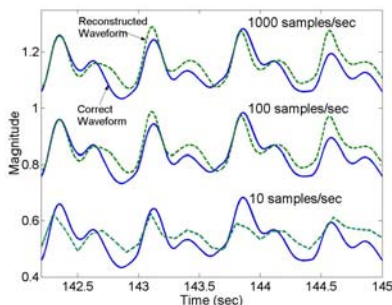


Fig. 13 Effects of sampling rate upon recovered PPG signal ( $n=10$ )

## VI. DISCUSSION

As can be seen in Figures 11(a) and 11(b), the additive distortion model gives promising results, as does the multiplicative/logarithmic model, which is based upon physical insight. It is believed that the idea of using a model based upon the physical system may be more useful

in the future in developing more robust wearable biosensors. Further, there are other filter options available for use, with the FIR model initially chosen for its simplicity. Future studies will also focus on exploring more robust filter models, attempting to minimize the number of parameters needed to estimate the distorted signal. In this way, the system will be better suited to real-time monitoring by decreasing algorithm computation time.

## VI. CONCLUSION

In this paper, a method to recover wearable sensor signals, corrupted due to body motion, has been presented. By using a MEMS accelerometer along with a PPG ring sensor, a low-order FIR model can be found relating PPG signal corruption to hand acceleration. This is done by use of an active noise cancellation algorithm in real-time.

Experiments have shown the ability to recover a corrupted PPG signal by using this algorithm with both an additive and multiplicative distortion model. Both methods have shown the ability to accurately reproduce PPG waveforms with distinct signal peaks from a corrupted PPG waveform. Thus, active noise cancellation using MEMS accelerometers is an effective method to produce motion-tolerant wearable sensors.

## ACKNOWLEDGMENT

This research has been conducted under a protocol approved by the Massachusetts Institute of Technology Committee On The Use of Humans as Experimental Subjects (Approval No. 3117).

Thanks to Hong-Hui Jiang and Levi Wood for their assistance with this paper.

## REFERENCES

- [1] Asada, H, Shaltis P, Reisner A, Rhee S, Hutchinson RC., "Wearable PPG-BioSensors", *IEEE Engineering in Medicine and Biology Magazine*, Vol.22, No.3, pp. 28-40, 2003.
- [2] Reisner, A., Shaltis, P., McCombie, D., and Asada, H., "A Critical Appraisal of Opportunities for Wearable Medical Sensors", *Proceedings of 2004 IEEE EMBS Conference*, 2004.
- [3] Aminian K, Robert P, Buchser EE, Rutschmann B, Hayoz D, Depairon M, "Physical activity monitoring based on acceletrometry: Validation and comparison with video observation", *Med Biol Eng Comput*, 37(3): 304-308, 1999.
- [4] Bussmann, J.B., J.H. Tulen, E.C. van Herel, and H.J. Stam, *Quantification of physical activities by means of ambulatory accelerometry: a validation study*. *Psychophysiology*, 35(5): p. 488-96, 1998.
- [5] Rhee, S-W., Yang, B-H, and Asada, H., "Artifact-Resistant, Power-Efficient Design of Finger-Ring Plethysmographic Sensors", *IEEE Transactions on Biomedical Engineering*, Vol.48, No.7, pp.795-805, July 2001.
- [6] Jiang, Hong-Hui, Asada, H. Harry, and Gibbs, Peter, "Active Noise Cancellation Using MEMS Accelerometers for Motion-Tolerant Wearable Biosensors", *Proceedings of 2004 IEEE EMBS Conference*, 2004.
- [7] Bergmann, Ludwig, and Schaefer, Clemens. *Optics of Waves and Particles*. Walter de Gruyter: New York, 1999. p.227
- [8] Bernard Widrow, Robert C. Goodlin et al., "Adaptive Noise Canceling: Principles and Applications", *Proceedings of the IEEE*, vol. 63, pp. 1692-1716, Dec.1975.